XLVI CILAMCE
VITÓRIA - ES - BRAZIL - 2025
XLVI IBERO-LATIN AMERICAN CONGRESS ON COMPUTATIONAL METHODS IN ENGENEERING

A study on the Radial Integration Method for elastoplastic analysis

Nathalia S. Manoel[1], Rodrigo G. Peixoto[1]

[1]*Post-Graduate Program in Structural Engineering, Federal University of Minas Gerais*
Av. Pres. Antônio Carlos, 6627 - Pampulha, 31270-901, Belo Horizonte - MG, Brazil
nathalia.smanoel@gmail.com, rodrigo.peixoto@dees.ufmg.br

Abstract. In the context of numerical analysis for structural engineering problems, the Boundary Element Method (BEM) offers a significant computational advantage by reducing problem dimensionality through boundary-only discretization. However, in elastoplastic problems, domain integrals arise, requiring special treatment. A widely adopted approach involves discretizing the domain into internal cells to evaluate these integrals, which, however, eliminates the primary advantage of dimensionality reduction. An alternative technique for handling domain integrals in nonlinear problems using BEM is the Radial Integration Method (RIM), which eliminates the need for domain discretization. In elastoplastic problems, the RIM transforms domain integrals into boundary integrals using a scheme of coordinates transformation and approximating initial stress increments by Radial Basis Functions (RBF) augmented with polynomial terms. In this study, the RIM is implemented to perform two and three-dimensional elastoplastic analysis. Numerical experiments demonstrate that this methodology maintains a reduced-order formulation in terms of dimensionality and achieves good results. It is shown that the use of only four integration points to evaluate the radial integrals, as cited in some literature texts, it is not sufficient. Moreover, a greater number of integration points become necessary as the boundary mesh is refined to avoid error propagation during the solution.

Keywords: Boundary Element Method, Elastoplasticity, Radial Integration Method

1 Introduction

According to Telles [1], the first publications on the treatment of elastoplastic materials can be attributed to Swedlow and Cruse [2], Mendelson [3] and Riccardella [4]. Considering the incomprehensibility of the tensor of plastic deformations, Mukherjee [5] verified some errors in the kernels involving inelastic fields for the case of a plane state of deformations and then Bui [6] presented the correct way to evaluate the derivatives of the singular integrals involving these inelastic terms, introducing new free terms. These results were applied to BEM by Telles and Brebbia [7].

Gao and Davies [8] define two of the most important tasks in the development of non-linear BEM as removing strong singularities that appear in domain integrals and solving the system equation. The authors briefly review historic research on these topics and provide novel methods to overcome these difficulties. Strongly singularities were treated using a semi-analytical method in which the domain integrals were performed through internal cell boundaries, while the system equations were solved using a Newton-Raphson algorithm based on the plastic multiplier.

Although the methodology developed by Gao and Davies [8] was effective in maintaining both accuracy and computational cost in terms of system solution, the cell approach is substantially more costly in terms of computational geometry modeling. Thus, the need for discretize the domain into cells was overcome by the Radial Integration Method proposed by Gao [10]. In this method, the domain integrals are directly transformed into equivalent boundary integrals without any domain discretization, except by the introduction of a set internal points.

Application of RIM to elastoplastic problems is firstly presented by Gao [10] in 2002. Only two simple examples (one of constant stress in a homogeneous cube under traction) are reported in this paper, and accordingly to the authors knowledge, no other works of elastoplastic analysis using RIM have been published after this. It is worth mentioning that both articles published by Gao [9] and [10] state that his experience shows that only four Gauss points are needed to achieve a highly accurate result. However, subsequent studies on the impact of numerical integration on the radial integral revealed that the number of integration points has a significant effect on

the accuracy of the results, thereby increasing the computational cost. In the application of the method to dynamic problems, Albuquerque et al. [11] drew attention to the possibility of improving accuracy at the expense of a larger computation time. Jesus et al. [12] and Doval et al. [13] investigated this issue in problems involving domain integrals with known variables. For viscous flow problems, a study was conducted involving approximation of unknown quantities, as detailed in Peng et al. [14].

In the present work, it is shown that the use of only four integration points to evaluate the radial integrals is not sufficient. Moreover, a greater number of integration points become necessary as the boundary mesh is refined to avoid error propagation during the solution.

2 Boundary Element Method for elastoplastic problems

Assuming a domain Ω within a boundary Γ with $\boldsymbol{\xi}$ and $\mathbf{x}$ as the source and the field points, respectively, the boundary integral equation for displacement in its incremental form can be expressed as:

$$c_{ij}(\boldsymbol{\xi})\dot{u}_j(\boldsymbol{\xi}) = \int_\Gamma u^*_{ij}(\boldsymbol{\xi},\mathbf{x})\dot{t}_j(\mathbf{x})d\Gamma(\mathbf{x}) - \int_\Gamma t^*_{ij}(\boldsymbol{\xi},\mathbf{x})\dot{u}_j(\mathbf{x})d\Gamma(\mathbf{x}) \quad + \int_\Omega \epsilon^*_{ijk}(\boldsymbol{\xi},\mathbf{x})\dot{\sigma}^p_{jk}(\mathbf{x})d\Omega(\mathbf{x}) \tag{1}$$

where $c_{ij}(\boldsymbol{\xi})$ is a parameter related to the boundary geometry around the source point $\boldsymbol{\xi}$, taken as $(1/2)\delta_{ij}$ for smooth boundary points and δ_{ij} for internal points. $\dot{t}_j(\mathbf{x})$, $\dot{u}_j(\mathbf{x})$ and $\dot{\sigma}^p_{jk}(\mathbf{x})$ represents the displacement, traction and initial stress incremental fields at the boundary Γ. $t^*_{ij}(\boldsymbol{\xi},\mathbf{x})$, $u^*_{ij}(\boldsymbol{\xi},\mathbf{x})$ and $\epsilon^*_{ijk}(\boldsymbol{\xi},\mathbf{x})$ are Kelvin's fundamental solutions for tractions and displacements components in j direction and strain components in jk direction at the field point $\mathbf{x}$ due to a unit concentrated load in i direction at the source point $\boldsymbol{\xi}$.

The initial stress increments $\dot{\sigma}^p_{ij}$ in eq. (1) can be related to the stress increments as:

$$\dot{\sigma}_{ij} = D^e_{ijkl}(\dot{\epsilon}_{kl} - \dot{\epsilon}^p_{kl}) = D^e_{ijkl}\frac{\partial \dot{u}_k}{\partial x_l} - \dot{\sigma}^p_{ij} \tag{2}$$

then, differentiating the displacements given in eq. (1) and using this relationship for interior nodes, the boundary integral equation for stress increments is obtained:

$$\dot{\sigma}_{ij}(\boldsymbol{\xi}) = \int_\Gamma u^*_{ijk}(\boldsymbol{\xi},\mathbf{x})\dot{t}_k(\mathbf{x})d\Gamma(\mathbf{x}) - \int_\Gamma t^*_{ijk}(\boldsymbol{\xi},\mathbf{x})\dot{u}_k(\mathbf{x})d\Gamma(\mathbf{x}) \quad + \int_\Omega \epsilon^*_{ijkl}(\boldsymbol{\xi},\mathbf{x})\dot{\sigma}^p_{kl}(\mathbf{x})d\Omega(\mathbf{x}) + F^\sigma_{ijkl}\dot{\sigma}^p_{kl}(\boldsymbol{\xi}) \tag{3}$$

where $t^*_{ijk}(\boldsymbol{\xi},\mathbf{x})$, $u^*_{ijk}(\boldsymbol{\xi},\mathbf{x})$ and $\epsilon^*_{ijkl}(\boldsymbol{\xi},\mathbf{x})$ are Kelvin's fundamental solutions and F^σ_{ijkl} is a free term originally verified by Bui [6].

Due to the hypersingular nature of the kernels that appears in eq. (3) at the boundary. The Traction Recovery Method (TRM) described, for example, in Gao and Davies [8] is adopted in this works to determine stress increments at boundary points:

$$\dot{\sigma}_{mn}(\boldsymbol{\xi}) = A_{mnj\alpha}\dot{u}^\alpha_j(\boldsymbol{\xi}) + B_{mnj}\dot{t}_j(\boldsymbol{\xi}) + C_{mnkl}\dot{\sigma}^p_{kl}(\boldsymbol{\xi}) \tag{4}$$

where $A_{mnj\alpha}, B_{mnj}, C_{mnkl}$ are coefficients that depend on geometry and material properties. $\dot{u}^\alpha_j(\boldsymbol{\xi})$, $\dot{t}_j(\boldsymbol{\xi})$ and $\dot{\sigma}^p_{kl}(\boldsymbol{\xi})$ correspond to the displacement, traction and initial stress incremental fields at the source point $\boldsymbol{\xi}$ at the boundary Γ. The α at the first term in the right side is related to the element shape functions.

3 Radial Integration Method

The Radial Integration Method (RIM) stipulates that the domain integration (Ω) of a function $f(\boldsymbol{\xi},\mathbf{x})$ can be transformed to a boundary integral (Γ). And, as defined by Gao [9], the RIM can be directly and accurately applied in domain integrals that contains known functions, while domain integrals with unknown variables must

be approximated with Radial Basis Functions (RBF), complemented (or not) by polynomial terms, before the application of the method.

In the equations stated in the previous section, the initial stress increments $\dot{\sigma}^p_{ij}(\mathbf{x})$ are unknown variables that can be approximated by:

$$\dot{\sigma}^p_{kl}(\mathbf{x}) \approx \sum_{A=1}^{N_A} a^A_{kl}\Phi_A(\mathbf{x}^A,\mathbf{x}) + c^0_{kl} + \sum_{i=1}^{\beta} c^i_{kl}x_i + \sum_{i=1}^{\beta}\sum_{j=1}^{\beta} c^{ij}_{kl}x_ix_j + \sum_{i=1}^{\beta}\sum_{j=1}^{\beta}\sum_{n=1}^{\beta} c^{ijn}_{kl}x_ix_jx_n + ... \tag{5}$$

where $\Phi_A(\mathbf{x}^A,\mathbf{x})$ are the RBF, which depend on the distance between an application point $\mathbf{x}^A$ to the field point $\mathbf{x}$, *i.e.*, $R = \|\mathbf{x}-\mathbf{x}^A\|$. N_A is the total number of application points and x_i are the Cartesian coordinates of an application point. $\beta = 2$ in two dimensions and $\beta = 3$ in three dimensions and $a^A_{kl}, c^0_{kl}, c^i_{kl}, c^{ij}_{kl}$ and c^{ijn}_{kl} are unknown coefficients.

Thus, using eq. (5), the domain integrals in eqs. (1) and (3) are transformed to boundary integrals using the RIM:

$$\int_\Omega \epsilon^*_{ijk}(\boldsymbol{\xi},\mathbf{x})\dot{\sigma}^p_{jk}(\mathbf{x})d\Omega(\mathbf{x}) = \quad \alpha^s_{jk}\int_\Gamma \epsilon^*_{ijk}(\boldsymbol{\xi},\mathbf{x})\frac{\partial r}{\partial n}F^s(\mathbf{x})d\Gamma(\mathbf{x}) \tag{6}$$

$$\int_\Omega \epsilon^*_{ijkl}(\boldsymbol{\xi},\mathbf{x})\dot{\sigma}^p_{kl}(\mathbf{x})d\Omega(\mathbf{x}) = \dot{\sigma}^p_{kl}(\boldsymbol{\xi})\int_\Gamma r\frac{\partial r}{\partial n}\ln(r)\epsilon^*_{ijkl}(\boldsymbol{\xi},\mathbf{x})d\Gamma(\mathbf{x}) + \quad \alpha^s_{kl}\int_\Gamma \epsilon^*_{ijkl}(\boldsymbol{\xi},\mathbf{x})r\frac{\partial r}{\partial n}\overline{F^s}(\mathbf{x})d\Gamma(\mathbf{x}) \tag{7}$$

where the radial integrals defined bellow arise:

$$F^s(\mathbf{x}) = \int_0^{r(\Gamma)} \Phi_A(\mathbf{x}^A,\mathbf{x})dr \quad \text{and} \quad \overline{F^s}(\mathbf{x}) \quad = \int_0^{r(\Gamma)} \frac{1}{r}\{\Phi_A(\mathbf{x}^A,\mathbf{x}) - \Phi_A(\mathbf{x}^A,\boldsymbol{\xi})\}dr \tag{8}$$

where $A \equiv s = 1, ..., N_s$, with $N_s = N_A + N_p$ and N_p corresponds to the number of polynomial terms.

Following Gao [10], the radial integrals in eq. (8) can be evaluated using standard Gauss quadrature.

4 Numerical examples

In this study, RIM was implemented in a pre-existent program that solves elastoplastic problems by BEM using cells. The radial integrals of the RBF terms in the initial stress approximation were evaluated using standard Gauss quadrature, while those associated with the polynomial terms were solved analytically.

In order to assess the accuracy of the method, two examples were solved assuming $\Phi_A(\mathbf{x}^A,\mathbf{x}) = \|\mathbf{x}-\mathbf{x}^A\| = R$, without polynomial terms (indicated as RBF only) and augmented with linear and quadratic polynomial terms. The cells results with quadratic interpolation of the initial stresses were obtained for each mesh considered with the points of the cell meshes taken as the application points for the RIM meshes. Cells and internal points were inserted exclusively within the expected plastic region. Additionally, due to the double symmetry, only a quarter of the problems was modeled.

4.1 Example 1 - Internally pressurized cylinder

The first example is a long metallic thick-walled cylinder (Fig. 1a) subject to internal pressure analyzed as a plane strain problem. Souza Neto et al. [15] approached this example whose analytic solution developed by Hill [16] for the plastic region, where $a \geq r \geq c$, is:

$$\sigma_{rr} = \frac{\sigma_{y0}}{\sqrt{3}}\left[-\frac{1}{2} - \ln\left(\frac{c}{r}\right) + \frac{c^2}{2b^2}\right] \text{ and } \sigma_{\theta\theta} = \frac{\sigma_{y0}}{\sqrt{3}}\left[\frac{1}{2} - \ln\left(\frac{c}{r}\right) + \frac{c^2}{2b^2}\right] \tag{9}$$

and, for the elastic region, where $c \geq r \geq b$, the solution is:

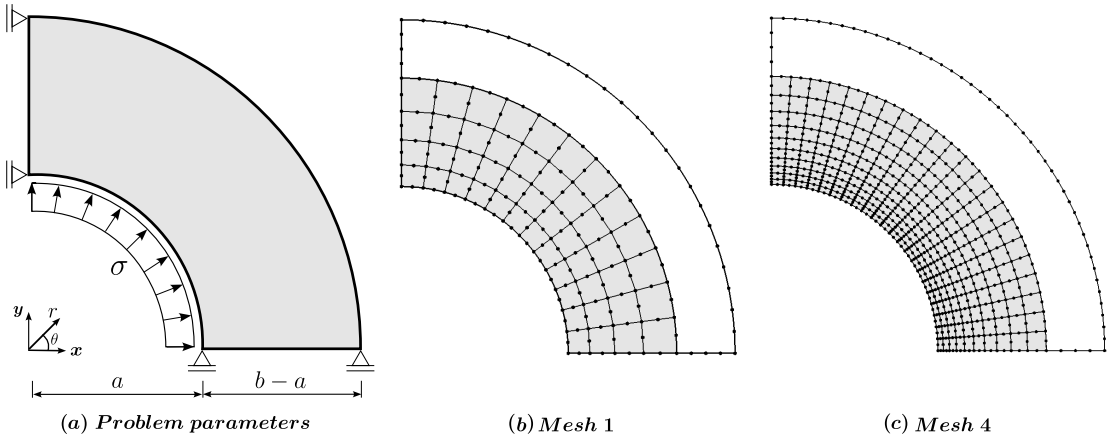
$$\sigma_{rr} = -\frac{\sigma_{y0}c^2}{2\sqrt{3}b^2}\left(\frac{b^2}{r^2} - 1\right) \text{ and } \sigma_{\theta\theta} = \frac{\sigma_{y0}c^2}{2\sqrt{3}b^2}\left(\frac{b^2}{r^2} + 1\right). \tag{10}$$

Additionally, the analytic expressions for the radial displacement (u_r) of the outer face before the plastic yielding starts is given by:

$$u_r = \frac{2\sigma b}{E(b^2/a^2 - 1)}(1 - \nu^2), \tag{11}$$

while under plastic yielding is:

$$u_r = \frac{\sigma_{y0}c^2}{\sqrt{3}Eb}(1 - \nu^2) \tag{12}$$



(a) *Problem parameters* (b) *Mesh* 1 (c) *Mesh* 4

Figure 1. Example 1 - Internally pressurized cylinder

In both solutions, a and b are the internal and external cyllinder's radius, respectively, and c is the radial distance from the origin to the limit of the plastic region. Here, the geometry was defined assuming a = 100 mm and b = 200 mm. The material properties has been taken as E = 210 GPa (Young's modulus), ν = 0.3 (Poisson ratio) and σ_{y0} = 0.24 GPa (yield limit), and a perfect plastic behavior with the von Mises criterion was adopted using 30 load increments. The internal pressure was taken as σ = 180 MPa which leads to a plastic region with $c \approx$ 159.79 mm. Fig. 1 illustrates boundary conditions of the problem and two of the meshes analyzed. The meshes analyzed were with 208, 372, 584 and 776 total points.

All meshes were analyzed using a fixed number of eight Gauss points for the boundary elements integration while the number of Gauss points for the radial integration (N_{gp}) varied between 8, 12 and 20. Table 1 shows the average percentage errors of domain results for the radial and hoop stresses across the domain as well as the radial displacement at the outer surface. Fig. 2 shows the plots of each numerical result of the table.

As can be seen from the plots, despite the small errors in the 208 and 372-point meshes, the results obtained with only eight Gaussian points are completely inaccurate for the more refined meshes. With 12 Gaussian points, the numerical results obtained with the 584-point mesh are good, but it is only with 20 Gaussian points that the more refined mesh shows adequate results.

From these results it is clear that the use of only 4 integration points in evaluation of radial integrals is not widely acceptable. Furthermore, as the mesh is refined, more integration points are required.

Table 1. Example 1 - Average percentage errors of domain results

		Mesh 1			Mesh 2			Mesh 3			Mesh 4		
	N_{gp}	σ_{rr}	$\sigma_{\theta\theta}$	u_{rr}	σ_{rr}	$\sigma_{\theta\theta}$	u_{rr}	σ_{rr}	$\sigma_{\theta\theta}$	u_r	σ_{rr}	$\sigma_{\theta\theta}$	u_{rr}
Cells	–	1.02	0.68	1.04	0.35	0.33	0.22	0.51	0.64	1.03	0.62	0.80	1.07
RBF only	8	1.12	0.80	0.76	0.70	0.55	0.50	190.32	382.69	101.49	120.43	154.85	20.49
	12	1.20	0.69	0.48	0.73	0.50	0.46	1.30	1.11	1.13	10.41	12.27	72.05
	20	1.19	0.69	0.51	0.67	0.47	0.41	0.58	0.64	1.32	0.61	0.66	1.99
Linear	8	1.19	0.79	0.74	0.72	0.57	0.76	163.01	302.94	115.06	8213.21	13001.30	2154.52
	12	1.26	0.68	0.50	0.76	0.50	0.43	1.38	1.16	1.02	5.61	6.12	38.68
	20	1.27	0.69	0.65	0.72	0.49	0.43	0.60	0.64	1.33	0.63	0.69	2.08
Quadratic	8	1.17	0.86	0.79	0.98	0.74	0.76	89.66	109.00	57.54	572.69	812.25	68.57
	12	1.28	0.78	0.88	0.72	0.50	0.44	1.96	1.59	0.80	6.27	7.42	57.91
	20	1.27	0.78	0.87	0.68	0.43	0.48	0.58	0.57	0.80	0.60	0.57	1.35

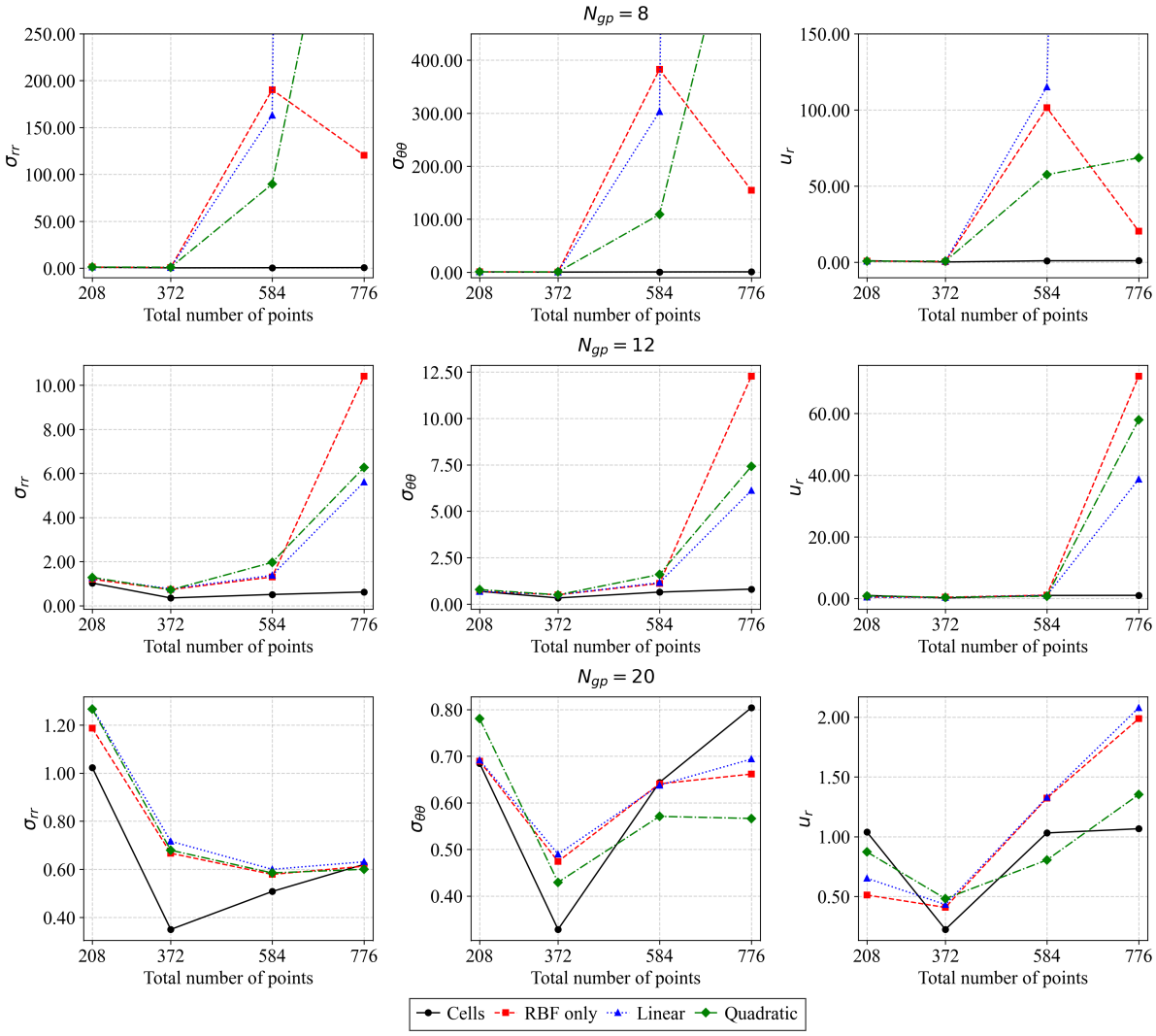


Figure 2. Example 1 - Average percentage errors of domain results

4.2 Example 2 - Tensile notched specimen

This second example is a plane stress analysis of a notched tensile specimen presented in Telles [1]. As for the mentioned reference, the material parameters adopted were $E = 7000$ kgf/mm, $\nu = 0.2$ and $\sigma_{y0} = 24.3$ kgf/mm, and a perfect plastic material was considered with the von Mises yield criterion. For this problem, a mesh with 280 total points was adopted with incremental load in 80 steps. Fig. 3.a depicted the geometric parameters, where $a = 5$ mm and $b = 18$ mm, and the mesh analyzed.

Similarly to the first example, a fixed number of four Gauss points was taken for the boundary integration, while four and eight Gauss points were assumed for the radial integration. Fig. 4 gives the load-displacement curves at point $P(18,0)$, which is depicted in Fig. 3.a.

As can be seen in the figure, four integration points leads to inaccurate load-displacement curves. On the other hand, increasing the number of integration points to eight provides a good correlation with the reference result, contrary to the initial assumption that only four points yield an accurate result. In this case, 20 Gaussian points were considered for radial integration, and it was observed that increasing the number of Gaussian points had a minimal impact on the results.

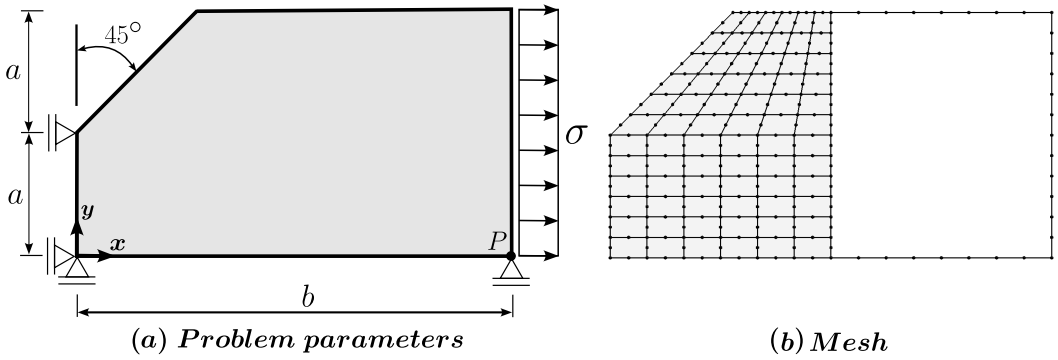


Figure 3. Example 2 - Tensile notched specimen

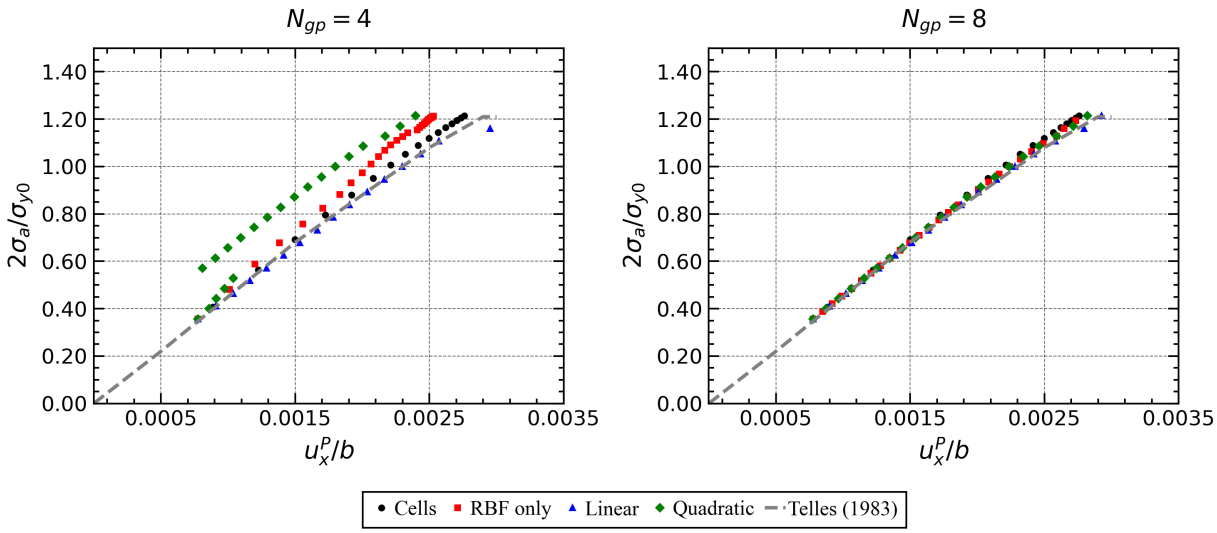


Figure 4. Example 2 - Load-displacement curves at point $P(18, 0)$ with 4 and 8 Gauss points for radial integration

5 Conclusions

The results obtained from the RIM for elastoplastic problems with the approximation of initial stress fields demonstrate that the method exhibits a high degree of accuracy. However, it is shown that the use of only four integration points to evaluate the radial integrals, as cited in some literature works, it is not sufficient. As illustrated in example 1 (section 4.1), an increase in the number of integration points for radial integrals is observed here to ensure the objectivity of the numerical analysis.

Acknowledgements. The autors gratefully acknowledge the financial support received from: CAPES - Coordenação de Aperfeiçoamento de Pessoal de Nível Superior; CNPq - Conselho Nacional de Desenvolvimento Científico e Tecnológico; and FAPEMIG - Fundação de Amparo à Pesquisa do Estado de Minas Gerais.

Authorship statement. The authors hereby confirm that they are the sole liable persons responsible for the authorship of this work, and that all material that has been herein included as part of the present paper is either the property (and authorship) of the authors, or has the permission of the owners to be included here.

References

[1] J. C. F. Telles. *The Boundary Element Method Applied to Inelastic Problems*, volume 1 of *Lecture Notes in Engineering*. Springer, 1983.
[2] J. L. Swedlow and T. A. Cruse. Formulation of boundary integral equations for three-dimensional elasto-plastic flow. vol. 7, n. 12, pp. 1673–1683, 1971.
[3] A. Mendelson. Boundary-integral methods in elasticity and plasticity. Tech report Nº E-7478, Nasa, 1973.
[4] P. C. Riccardella. An Implementation of the Boundary-integral Technique for Planar Problems in Elasticity and Elasto-plasticity, 1973.
[5] S. Mukherjee. Corrected boundary-integral equations in planar thermoelastoplasticity. vol. 13, n. 4, pp. 331–335, 1977.
[6] H. D. Bui. Some remarks about the formulation of three-dimensional thermoelastoplastic problems by integral equations. vol. 14, n. 11, pp. 935–939, 1978.
[7] J. C. F. Telles and C. A. Brebbia. On the application of the boundary element method to plasticity. vol. 3, n. 6, pp. 466–470, 1979.
[8] X.-W. Gao and T. G. Davies. An effective boundary element algorithm for 2D and 3D elastoplastic problems. vol. 37, n. 36, pp. 4987–5008, 2000.
[9] X.-W. Gao. The radial integration method for evaluation of domain integrals with boundary-only discretization. *Engineering Analysis with Boundary Elements*, vol. 26, n. 10, pp. 905–916, 2002a.
[10] X.-W. Gao. A Boundary Element Method Without Internal Cells for Two-Dimensional and Three-Dimensional Elastoplastic Problems . *Journal of Applied Mechanics*, vol. 69, n. 2, pp. 154–160, 2002b.
[11] E. Albuquerque, P. Sollero, and Portilho de W. Paiva. The radial integration method applied to dynamic problems of anisotropic plates. *Communications in Numerical Methods in Engineering*, vol. 23, n. 9, pp. 805–818, 2007.
[12] L. J. Jesus, E. L. Albuquerque, and P. Sollero. Further development in the radial integration method. *Mecánica Computacional*, vol. 29, n. 55, pp. 5567–5575, 2010.
[13] P. Doval, E. Albuquerque, P. Sollero, and others. Numerical aspects of the radial integration method in boundary element formulation for stability analysis of thin perforated plates of laminated composites. *Blucher Mechanical Engineering Proceedings*, vol. 1, n. 1, pp. 3879–3887, 2012.
[14] H.-F. Peng, M. Cui, and X.-W. Gao. A boundary element method without internal cells for solving viscous flow problems. *Engineering Analysis with Boundary Elements*, vol. 37, n. 2, pp. 293–300, 2013.
[15] E. A. Souza Neto, D. Peric, and D. R. J. Owen. *Computational methods for plasticity: theory and applications*. John Wiley & Sons, 2008.
[16] R. Hill. *The Mathematical Theory of Plasticity*. Oxford Classic Texts in the Physical Sciences. Oxford University Press, 1950.